ISSN 1063-7729, Astronomy Reports, 2011, Vol. 55, No. 7, pp. 616–621. © Pleiades Publishing, Ltd., 2011.
Original Russian Text © T.G. Sitnik, 2011, published in Astronomicheskii Zhurnal, 2011, Vol. 88, No. 7, pp. 671–676.

Structure and Kinematics of the ISM Near WR 139

T. G. Sitnik

Sternberg Astronomical Institute, Universitetskii pr. 13, Moscow, 119234 Russia

Received September 3, 2010

Abstract—The structure and kinematics of the ISM in an extended vicinity of the star WR 139 is analyzed using the results of original Hα interferometric observations together with radio and infrared data. A CO cavity with a size of up to 40′ has been detected around the star at velocities of $V_{\rm LSR} \sim 2.5-10$ km/s; the cavity is bounded to the North by a shell radiating in the optical. Ionized hydrogen emits at the systematic velocities $V_{\rm LSR} \sim 6-14$ km/s toward the CO cavity, and at $V_{\rm LSR} \simeq 4-11$ km/s toward the shell. High-velocity motions of ionized hydrogen inside the cavity testify to the probable expansion of gas that has been swept out by the stellar wind of WR 139 at velocities of up to 60–80 km/s.

DOI: 10.1134/S1063772911060072

1. INTRODUCTION

We study here the ISM (ISM) in a broad vicinity of the star WR 139 ($\alpha_{2000} \sim 20^{\rm h}16^{\rm m}-20^{\rm h}23^{\rm m}$, $\delta_{2000} \sim 38^\circ-39^\circ35'$) based on the results of a long-term program of Hα interferometric observations of the Cygnus gas-dust complex [1] (see also references therein). The purpose of this work was to search for signs of the influence of stellar winds on the structure and kinematics of the ISM. The high-velocity stellar wind interacting with the two-phase ISM creates shock fronts that propagate in the rarefied gas and in molecular clouds [2]. An expanding interstellar bubble—a hot cavity surrounded by a shell of swept out interstellar material—is formed in the vicinity of the star [3, 4].

The star WR 139 (V444 Cyg, HD 193576) is a WN5 + O6 binary system. It is a probable member of the open cluster Be 86 and the Cyg OB1 association [5, 6] (Fig. 1). The distance to the cluster and association is 1.5 kpc [5, 9]. The interstellar extinction toward the star is taken to be $A_v = 2.83^m$ in [6]. The star is projected inside a shell around the Cyg OB1 and Cyg OB3 associations. The shell has been observed in the optical, radio, and infrared [10–13]. Heckathorn et al. [14] suggest that the optical emission 15′–50′ North of WR 139 is probably due to this star (Fig. 1). Miller and Chu [8] found a diffuse nebula in Hα + [N II] in the immediate vicinity of the star (within 6′). The kinematics of the ionized hydrogen around WR 139 have not been studied earlier.

The results of our Hα observations are presented in Section 2. In Sections 3 and 4, we study the structure and kinematics of the ISM around WR 139 and search for signs of the expansion of the interstellar gas. Our results are summarized in Section 5.

2. KINEMATICS OF IONIZED HYDROGEN

We studied the kinematics of the ionized gas in an extended region around WR 139 using the results of our Hα observations. These data were obtained with a Fabry–Perot interferometer at the Cassegrain focus of the 125-cm reflector of the Crimean Laboratory of the Sternberg Astronomical Institute. The field of view and angular resolution were 10′ and 3″–4″, respectively; the actual spectral resolution was $\simeq$10–15 km/s. The line profile was approximated by one or several Gaussians, assuming that the half-width of each component should exceed the half-width of the instrumental profile and that the signal-to-noise ratio is $\geq$5. The velocities were determined at the maximum of each peak of the profile. (The observing and reduction techniques are described in detail in [1]; see also references therein). In 1995–2000, we obtained more than 70 plates, which we used to estimate more than 1800 radial velocities in various parts of the studied region. Our observations cover the region nonuniformly: we have studied regions with bright optical features or those in which high-velocity components were detected in Hα most thoroughly.

Multi-peaked Hα profiles are observed in the broad vicinity of WR 139, as everywhere toward the Cygnus Complex. These consist of one or more bright main components within $V_{\rm LSR} \sim \pm20$ km/s, characterizing the unshifted gas and faint shifted components in the line wings out to $V_{\rm LSR} \sim \pm80$ km/s.

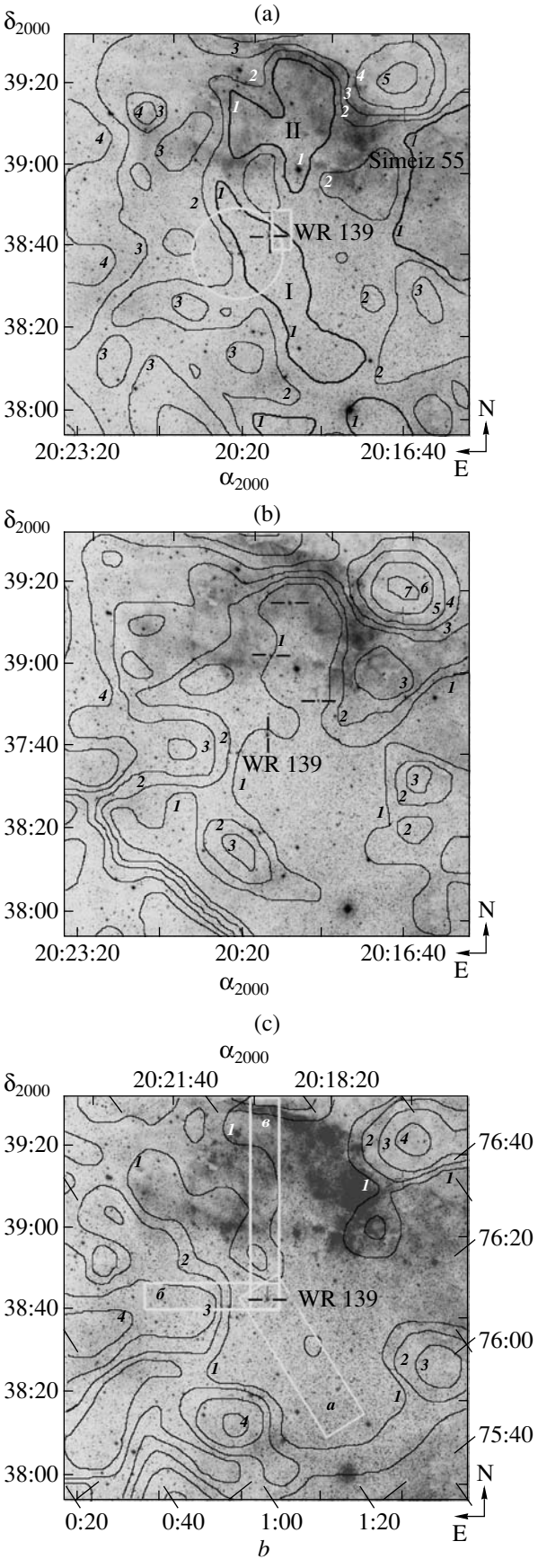

The radial velocities of the main Hα component describe systematic large-scale motions associated with the Galactic rotation and spiral-density shocks. In the case of pure differential Galactic rotation, the radial velocities of the Cygnus-Arm population in the studied direction lie within 7–10 km/s [15]. This is smaller than the observed velocity interval, which also includes "forbidden" negative values. In this case, broadening of the radial-velocity range of the gas in the Cygnus Arm is due to variations in the velocities of azimuthal gas flows in the arm cross-section [16] (see also references therein).

The radial velocities of the shifted Hα components characterize local high-velocity gas motions formed by supernova explosions or stellar winds from objects in the Cygnus Arm. Distant H II regions of the Perseus Arm may contribute at large negative velocities.

To find the characteristic velocities of ionized hydrogen in various parts of the region studied, we plotted radial-velocity histograms for the directions in which features are observed in the distribution of the CO and Hα emission (such as H II regions, interstellar clouds, or cavities). We used these graphs to determine the mean radial velocities $V_{\rm LSR}$ characteristic of each region, together with their rms errors Δ. The characteristic radial velocity $\langle V_{\rm LSR}\rangle$ was determined as the mean at the half maximum of the corresponding graph. The results are listed in the Table, whose rows contain the region number, its equatorial or Galactic coordinates, the number of points in which the radial velocities were measured N_1, the range of the most frequently observed radial velocities $(\langle V_{\rm LSR}\rangle - \Delta)$–$(\langle V_{\rm LSR}\rangle + \Delta)$, with systematic velocities in boldface, the number of measurements from which the velocity range was determined N_2, and a description of the region. Several velocity ranges at the same position testify to the presence of

Fig. 1. Vicinity of the star WR 139 (red map). (a) CO emission [7] in a broad velocity range, $V_{\rm LSR} \simeq$ from −25 to 25 km/s. Regions are labeled with numbers in order of increasing brightness, with *1* corresponding to the faintest region. The Roman numerals I and II mark regions devoid of CO emission (inside contour *1*); the region in which a diffuse nebula radiating in the Hα +[N II] lines was detected [8] is outlined with a white rectangle. The star WR 139, nebula Simeiz 55, and cluster Be 86 (inside a circle) are marked. (b) Contours of CO emission in the range $V_{\rm LSR} \simeq 2.5$–5 km/s [7]. The CO cavity is bounded by the contour *1*. WR 139 and the O stars HD 193595, HD 228841, and HIP 100173 at the North of the region are marked. (c) Contours of CO emission in the range $V_{\rm LSR} \simeq 5$–7.5 km/s [7]. The CO cavity is bounded by the contour *1*. The regions for which P/V diagrams were plotted are shown with rectangles.

Radial velocities of ionized hydrogen V_{LSR}

No.	$\alpha_{2000}, \delta_{2000}$ (Nos. 1–6) l, b (Nos. 7, 8)	N_1	$(V_{LSR} - \Delta) \ldots (V_{LSR} + \Delta)$, km/s	N_2	Region
1	$20^h15^m40^s$–$20^h17^m20^s$	173	−54 . . . − 36	42	The nebula Simeiz 55
	38°50′–39°10′		**3–7**	78	
			37–53	21	
2	20 17 00–20 20 00	230	−60 . . . − 50	12	WR 139, southern part of the CO cavity
	38 20–38 45		−32 . . . − 20	28	
			6–14	147	
3	20 17 20–20 22 20	520	−44 . . . − 32	56	Shell observed
	38 57–39 35		**4–10**	351	in the [O III], Hα + [N II] and [S II] lines
			37–51	18	
4	20 18 00–20 19 30	353	−35 . . . − 27	33	WR 139, northern part of the CO cavity
	38 40–39 30		**4–10**	206	
			35–53	14	
5	20 18 00–20 20 00	82	−54 . . . − 40	10	Northern filament
	39 22–39 36		**3–7**	51	
			36–56	5	
6	20 19 00–20 19 30	81	−77 . . . − 75	3	Diffuse nebula [8] (within
	38 38–38 50		−33 . . . − 21	12	the rectangle in Fig. 1a)
			6–14	16	
7	75°58′ – 76°55′	329	−61 . . . − 51	19	Region I in Fig. 1a
	1°16′ – 1°30′		−32 . . . − 16	51	
			6–14	182	
			46–50	7	
8	76 40 00–77 10 00	291	−40 . . . − 30	25	Region II in Fig. 1a
	1 30–1 58		**5–11**	180	
			37–53	13	

several maxima in histogram. Because of incomplete coverage of our observations, the existence of a maximum of high-velocity components does not imply the dominance of motions in the given velocity range; instead, this only ascertains the existence of motions with such velocities.

It follows from the Table that ionized hydrogen in the studied part of the Cygnus Arm moves at the systematic velocities $V_{LSR} \simeq 4$–14 km/s. In some northern regions (e.g., the bright northern filament and the nebula Simeiz 55), motions in a narrower velocity interval $V_{LSR} \simeq 3$–7 km/s are observed. The same velocities, $V_{LSR} \simeq 2.5$–7.5 km/s, are observed in the northern molecular clouds [7] (see also Figs. 1b, 1c). The H II velocities to the West of WR 139, in the diffuse nebula [8], are $V_{LSR} \simeq 6$–14 km/s. The derived radial velocities of the main Hα component are characteristic of the Cygnus-Arm population. They are consistent with the velocities of molecular clouds of this arm in the studied direction [17] (see also [18, Fig. 2]).

An analysis of the high-velocity component of the Hα line aimed at searching for the effects of the stellar wind from WR 139 on the surrounding gas is carried out in Section 4.

3. THE ISM AROUND WR 139

The analysis of our Hα observations, narrow-band optical-line observations [8, 19], CO observations [7], and infrared emission (IRAS and Spitzer/IRAC [20] data) has led us to draw the following conclusions about the ISM around WR 139:

1. The star is projected against a region in which CO emission is absent in a broad velocity range, $V_{\rm LSR} \simeq$ from −25 to 25 km/s; i.e., throughout the Cygnus Arm (region I inside the contour *1* in Fig. 1a). Since the systematic radial velocities of the ionized hydrogen near WR 139 are $V_{\rm LSR} \simeq 6-14$ km/s, we considered the distribution of the CO emission in this velocity interval and detected a CO cavity with a size of up to 40′ at $V_{\rm LSR} \simeq 2.5-10$ km/s. Figures 1b, 1c present contours of the CO emission in two velocity intervals, $V_{\rm LSR} \simeq 2.5-5$ km/s and $V_{\rm LSR} \simeq 5-7.5$ km/s. Figure 1c shows that the molecular clouds close to WR 139 are at projected distances of 0.1° (3 pc) to the North and East and 0.6° (16 pc) to the Southwest. There are no molecular clouds to the West of the cavity; rare small clouds are visible at $V_{\rm LSR} > 10$ km/s [7].

2. The emission shell around WR 139 can be traced by bright emission in the [O III], Hα + [N II], and [S II] lines 15′−50′ (8–28 pc) to the North of the star [19] and by faint emission in the Hα + [N II] lines within 6′ to the West (Fig. 1a; see also [8, Fig. 1]). As in the close vicinity of WR 139 (region I), bright emission to the North (region II within contour *1*) and faint emission near the star (within the rectangle in Fig. 1a) are visible in gaps between foreground molecular clouds. Unshifted ionized hydrogen in these regions radiates at the same systematic velocities, $V_{\rm LSR} \simeq 5-11$ km/s and $V_{\rm LSR} \simeq 6-14$ km/s, as ionized gas near WR 139 in region I (table). A connection of the complex of northern nebulae with WR 139 is also supported by the bright emission in the [O III] lines and the fine filamentary Hα + [N II] structure at the CO cavity boundary. However, the optical emission observed to the North cannot be associated with WR 139 alone. Several O stars are projected against this region (Fig. 1b) they contribute to forming the northern nebulae. Furthermore, the entire complex of northern H II regions is part of a large-scale shell around the Cyg OB1 and Cyg OB3 associations [10]. As noted above, precisely this part displays bright [O III] emission [19].

3. There is virtually no heated dust (IRAS 60 and 100 μm, MIPS 24 μm) in the vicinity of WR 139, at least within region I. The absence of dust that could be swept out by the wind from WR 139 is consistent with the CO cavity detected around the star. Instead, dust (MIPS 24 μm) is visible toward the optical shell to the North, and bright infrared emission at 8, 5.8, and 3.6 μm was detected at its periphery [20]. This emission is part of a large-scale infrared shell around the Cyg OB1 and Cyg OB3 (and, probably, Cyg OB9) associations, detected earlier in the 60 and 100 μm bands [11, 12].

Thus, there is a region of reduced CO, Hα, and infrared emission near WR 139. The CO cavity around the star is prominent at the systematic velocities $V_{\rm LSR} \simeq 2.5-10$ km/s. The optical shell is visible in gaps between foreground molecular clouds (Fig. 1a). Ionized hydrogen near WR 139 (region I) and in the shell radiates in the overlapping velocity intervals $V_{\rm LSR} \simeq 6-14$ km/s and $V_{\rm LSR} \simeq 4-10$ km/s.

With regard to the structure of the ISM around WR 139, the expansion of the shell detected from faint features in the Hα wings should be searched for in first instance in the region devoid of foreground absorbing clouds, i.e., in region I (Fig. 1a).

4. HIGH-VELOCITY MOTIONS NEAR WR 139

To reveal the kinematic effects of the wind from WR 139 on the surrounding gas, we analyzed faint high-velocity Hα components. If the surrounding gas is swept out by the stellar wind, the radial velocities of the shifted H II components should decrease radially in magnitude to the systematic velocity, demonstrating so-called "radial-velocity ellipses." To detect these, we plotted P/V diagrams—distributions of the radial velocities versus the projected distance from the star. To minimize the effect of the complex structure of the ISM and of other stellar-wind sources, we plotted graphs in the directions shown in Fig. 1c. The P/V diagrams to the Southwest, East, and North of WR 139 are presented in Figs. 2a, 2b, 2c, respectively.

Figure 2 shows that the radial-velocity ellipses are traced by the variations of the extreme values of $V_{\rm LSR}$ in all the studied directions. The high H II velocities (from −80 to −60 km/s) decrease in magnitude to the velocity of the surrounding medium at projected distances 0.1°−0.6°. In each direction, this distance coincides with the distance to the closest molecular clouds (Figs. 1c, 2). The diffuse nebula [8] is observed within the smallest of these distances. Note especially the southwest direction, along the plane of the Galaxy (Fig. 2a): here, the size of the region in which the radial velocity of the perturbed gas becomes equal to that of the surrounding medium is the largest of those considered, consistent with the fact that the largest extent of region I and the CO cavity is in this direction.

The described radial-velocity behavior can be interpreted as expansion of the gas swept out by the

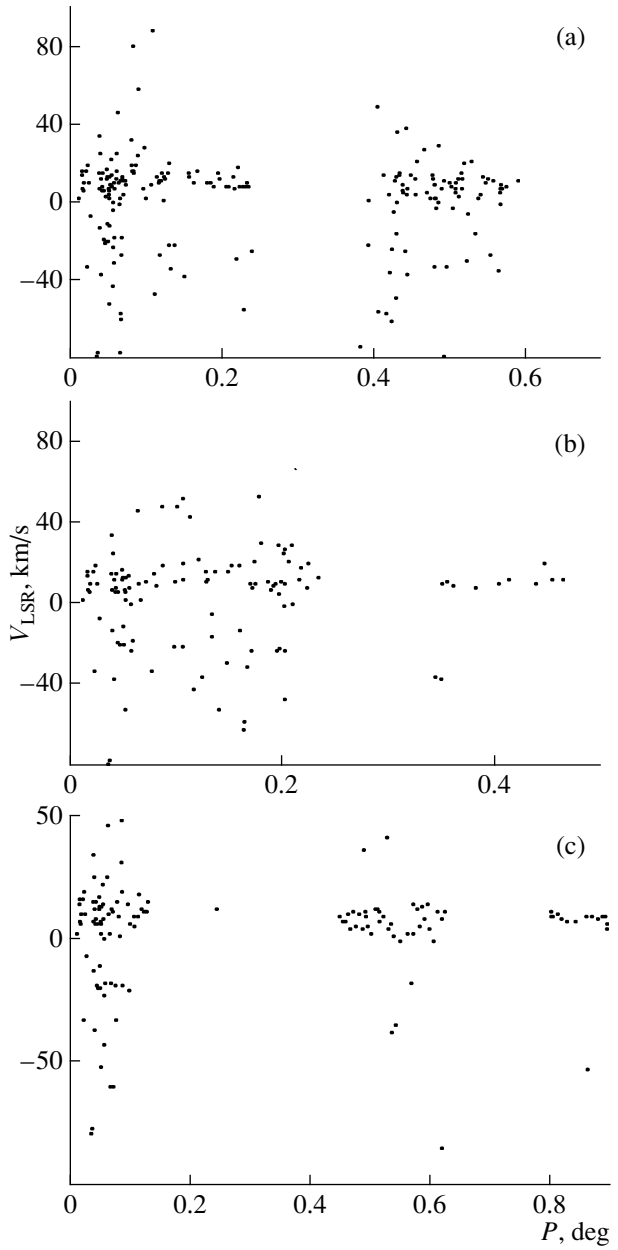

Fig. 2. P/V diagram in the vicinity of WR 139 for the regions indicated in Fig. 1c in the (a) southwestern, (b) eastern, and (c) northern directions.

wind of WR 139 at velocities of up to 60–80 km/s. (Note that the main unshifted velocity component in Fig. 2 includes emission of unperturbed gas near the star and in the line of sight.)

Thus, the ionized hydrogen observed in gaps between molecular clouds of the Cygnus Arm is swept out by the wind of WR 139 at velocities reaching 60–80 km/s. The fact that the high-velocity motions terminate in the molecular clouds around the cavity may testify to a physical connection of WR 139 with the cavity.

5. CONCLUSION

We have found indications of the influence of stellar wind on the ISM in the neighborhood of WR 139. At $V_{LSR} \simeq 2.5-10$ km/s, we detected a CO cavity with a size of up to 40′. The ionized hydrogen in this cavity radiates at the systematic velocities $V_{LSR} \sim 6-14$ km/s. A probable shell around WR 139 is observed at the northern periphery of the CO cavity, as bright emission in the [O III], Hα + [N II], and [S II] lines, both diffuse and with a fine filamentary structure characteristic of shock waves. In the vicinity of the star, we found an extended region (region I) $15' \times 60'$ in size that is devoid of CO emission and appreciable optical emission along the entire extent of the Cygnus Arm. We have found expansion of ionized hydrogen under the action of the wind of WR 139 at velocities reaching 60–80 km/s through this gap in the foreground absorbing clouds. The emission shell to the North and the immediate vicinity of the star are visible in a gap between molecular clouds (region II in Fig. 1a). Unshifted ionized hydrogen is observed in this region and in the northwest part of the shell (diffuse nebula), within the same velocity interval as near WR 139 (region I).

According to [6], WR 139 may be a member of the cluster Be 86 and association Cyg OB1; therefore, it is possible that the gas is expanding due to the action of the stellar wind in a "pre-prepared" complex-shaped cavity formed by the combined action of the wind and ionizing radiation of the stars of these groups. In this case, the wind of WR 139 is propagating in a low-density medium, and the emission of its own shell may be below the detection threshold; this is probably observed to the South of the cavity. The optical emission to the North of WR 139, which we consider to be a probable shell formed by the stellar wind, following [6, 14], is also part of a large-scale shell detected in the optical, radio, and infrared around Cyg OB1, Cyg OB3, and, probably, Cyg OB9.

As a whole it is fairly difficult to observe the gas expansion. The numerous sources of shocks (the line of sight passes along the Cygnus Arm, at least within 3 kpc), foreground absorbing clouds, low density of the ISM, and low sensitivity of the instrumentation hinder detection of the gas expansion.

Our results are consistent with other studies of the region. According to the distribution of interstellar extinction [5, Fig. 9], WR 139 is at the periphery of a layer of absorbing clouds concentrated toward the plane of the Galaxy. This is consistent with the detected CO cavity, which is bounded by clouds on the side of the Galactic plane and is open toward higher Galactic latitudes. The diffuse nebula detected

in [8] lies within the minimum distance where the expansion of ionized hydrogen in the vicinity of WR 139 was found.

ACKNOWLEDGMENTS

This work is based interferometric Hα observations on the 125-cm reflector of the Crimean Laboratory, Sternberg Astronomical Institute, Moscow State University. This research has made use of the SIMBAD database, Centre de Données astronomiques (Strasbourg, France). This work was supported by the Russian Foundation for Basic Research (project no. 10-02-00091).

REFERENCES

1. T. A. Lozinskaya, V. V. Pravdikova, and T. G. Sitnik, et al., Astron. Zh. **75**, 514 (1998) [Astron. Rep. **42**, 453 (1998)].
2. K. V. Bychkov and S. B. Pikelner, Pis'ma Astron. Zh. **1**, 29 (1975).
3. J. Castor, R. McCray, and R. Weaver, Astrophys. J. Lett. **200**, 107 (1975).
4. R. Weaver, R. McCray, J. Casto, et al., Astrophys. J. **218**, 377 (1977).
5. D. Forbes, D. English, M. M. De Robertis, and P. C. Dawson, Astron. J. **103**, 916 (1992).
6. K. A. van den Huhcht, New Astron. Rev. **45**, 135 (2001).
7. H. O. Leung and P. Thaddeus, Astrophys. J. Suppl. Ser. **81**, 267 (1992).
8. G. J. Miller and Y. H. Chu, Astron. Astrophys. Suppl. Ser. **85**, 137 (1993).
9. C. D. Garmany and R. E. Stencel, Astron. Astrophys. Suppl. Ser. **94**, 214 (1992).
10. T. A. Lozinskaya and T. G. Sitnik, Pis'ma Astron. Zh. **14**, 240 (1988) [Sov. Astron. Lett. **14**, 100 (1988)].
11. T. A. Lozinskaya and S. N. Repin, Pis'ma Astron. Zh. **17**, 1152 (1991).
12. J. M. Saken, J. M. Shull, C. D. Garmany, et al., Astrophys. J. Lett. **397**, 537 (1992).
13. P. E. Dewdney and T. A. Lozinskaya, Astron. J. **108**, 2212 (1994).
14. J. N. Heckathorn, F. C. Bruhweiler, and T. R. Gull, Astrophys. J. **252**, 230 (1982).
15. A. K. Dambis, A. M. Mel'nik, and A. S. Rastorguev, Pis'ma Astron. Zh. **21**, 331 (1995) [Astron. Lett. **21**, 291 (1995)].
16. T. G. Sitnik, A. M. Mel'nik, and V. V. Pravdikova, Astron. Zh. **78**, 40 (2001) [Astron. Rep. **45**, 34 (2001)].
17. T. M. Dame, D. Hartmann, and P. Thaddeus, Astrophys. J. **547**, 792 (2001).
18. T. G. Sitnik and T. A. Lozinskaya, Pis'ma Astron. Zh. **35**, 137 (2009) [Astron. Lett. **35**, 121 (2009)].
19. R. A. P. Parker, T. R. Gull, and R. P. Kirshner, Preprint NASA SP-434 (NASA, Washington, 1979).
20. J. L. Hora (and The Cygnus-X Legacy Team), in *New Light on Young Stars: Spitzer's View of Circumstellar Disks, Proeedings of the 5th Spitzer Conference, Oct. 26–30, 2008, Pasadena, CA, CalTech,* http://www.ipac.caltech.edu/spitzer2008/talks/JosephHora_Spitzer2008Conference.pdf(2008).

Translated by G. Rudnitskii